Combined Simulation and Mutation Studies to Elucidate Selectivity of Unsubstituted Amphetamine-like Cathinones at the Dopamine Transporter

Amir Seddik,[a] Daan P. Geerke,[b] Thomas Stockner,[c] Marion Holy,[c] Oliver Kudlacek,[c] Nicholas V. Cozzi,[d] Arnold E. Ruoho,[e] Harald H. Sitte,[c] and Gerhard F. Ecker*[a]

Abstract: The dopamine and serotonin transporter proteins (DAT, SERT) play a vital role in behavior and mental illness. Although their substrate transport has been studied extensively, the molecular basis of their selectivity is not completely understood yet. In this study, we exploit molecular dynamics simulations combined with mutagenesis studies to shed light on the driving factors for DAT-over-SERT selectivity of a set of cathinones. Results indicate that these compounds can adopt two binding modes of which one is more favorable. In addition, free energy calculations indicated the substrate binding site (S1) as the primary recognition site for these ligands. By simulating DAT with SERT-like mutations, we hypothesize unsubstituted cathinones to bind more favorably to DAT, due to a Val152 offering more space, as compared to the bulkier Ile172 in SERT. This was supported by uptake inhibition measurements, which showed an increase in activity in SERT-I172V.

Keywords: monoamine transporters · docking · molecular dynamics · thermodynamic integration · uptake inhibitory assay

1 Introduction

The dopamine and serotonin transporter (DAT and SERT, respectively) are part of the neurotransmitter:sodium symporter (NSS) subfamily. They exert their action by re-uptaking neurotransmitter molecules back into the synaptic cleft using the electrochemical gradient of sodium ions. Despite their high structural similarity, SERT and DAT are implicated in different behavior and mental illnesses: SERT has mostly been associated with depression,[1] anxiety,[2] and obsessive-compulsive disorder,[3] while mutations in DAT have been linked to e.g. attention-deficit hyperactivity disorder.[4,5] Although these transporters are established targets for numerous drugs, the molecular determinants for their ligand selectivity are not completely understood yet.[6,7,8]

Cathinones are ligands for SERT and DAT and represent a class of drugs used to treat various medical conditions including depression,[9] obesity,[10] and muscle spasms.[11] However, they are also used as street drugs causing many health and addiction problems.[12] Understanding the molecular basis of their activity and selectivity on monoamine transporters may therefore pave the way for the design of compounds with less potential for abuse. We previously showed that SERT-over-DAT selectivity of cathinones is driven by polarizable or lipophilic *para*-substituents.[13] In contrast, the molecular basis for DAT-over-SERT selectivity is not fully grasped. Our previous efforts on the 'second generation' mephedrone analog 4′-methyl-α-pyrrolidinopropiophenone (4-MePPP) have indicated that cathinones comprising a bulky *N*-substituent are DAT selective due to a lack of space in the *B* sub pocket, which is part of the substrate binding site (S1). However, amphetamines lacking substituents on their aromatic ring tend to be DAT-over-SERT selective as well, an observation that has not been explained so far.[8,13]

[a] A. Seddik, G. F. Ecker
University of Vienna, Department of Pharmaceutical Chemistry, Althanstrasse 14, 1090 Vienna, Austria
*e-mail: gerhard.f.ecker@univie.ac.at

[b] D. P. Geerke
AIMMS Division of Molecular Toxicology, Department of Chemistry and Pharmaceutical Sciences, VU University, De Boelelaan 1083, 1081 HV Amsterdam, the Netherlands

[c] T. Stockner, M. Holy, O. Kudlacek, H. H. Sitte
Medical University of Vienna, Institute of Pharmacology, Center for Physiology and Pharmacology, Währingerstrasse 13a, 1090 Vienna, Austria

[d] N. V. Cozzi
Department of Cell and Regenerative Biology, University of Wisconsin School of Medicine and Public Health, 1300 University Avenue, Madison, WI 53706

[e] A. E. Ruoho
Department of Neuroscience, University of Wisconsin School of Medicine and Public Health, 1300 University Avenue, Madison, WI 53706

💻 Supporting information for this article is available on the WWW under http://dx.doi.org/10.1002/minf.201600094.

In this study, we exploit differences in uptake inhibitory activity of these small substrates via a combined computational and experimental approach in order to explore the basis for their DAT-over-SERT selectivity.

2 Materials and Methods

2.1 Drugs and Reagents

Reagents used in the experiments for uptake assays in cells were purchased and used according to previous work.[14] Plasmids encoding human SERT were a generous gift of Dr. Randy D. Blakely and used in a tagged form.[15]

2.2 Synthesis of 4-IMAP

4-iodomethcathinone (1-[4-iodophenyl]-2-[methylamino]-propan-1-one; 4-IMAP) was synthesized from 4-bromo-methcathinone (4-BMAP; synthesized as described in Ref.[16]) via a two-step stannylation-iodination reaction. Briefly, a solution of 4-BMAP (1 eq.), hexabutyldistannane (2 eq.), and tetrakis(triphenylphosphine)palladium (0.05 eq.) in dry toluene was refluxed for 90 min, after which time the reaction was essentially complete by TLC (silica gel, CH_2Cl_2:MeOH 4:1). The mixture was cooled, filtered, and concentrated *in vacuo*, then the product 4-tributylstannyl-methcathinone (i.e. 2-[methylamino]-1-[4-(tributylstannyl)-phenyl]propan-1-one) was purified by column chromatography (silica gel; CH_2Cl_2:MeOH, 4:1). The fractions containing the desired product were combined and concentrated *in vacuo*. ^{1}H-NMR analysis of the resulting brown oil was consistent with the expected product. Iodination of the purified tributylstannyl intermediate was performed by incubating the brown oil with NaI and 3% H_2O_2 in NaOAc buffer, pH = 4.2 for 15 min. After quenching the reaction with 3 M $NaHSO_3$ the mixture was made basic with 5 M NaOH, extracted with CH_2Cl_2, and concentrated *in vacuo*. The resulting oily free-base 4-IMAP was crystallized from diethyl ether as the hydrochloride salt. The identity of 4-IMAP was confirmed with ^{1}H-NMR and elemental analysis.

2.3 Ligand Preparation

Two cathinone type ligands from an *in-house* dataset[13] were selected to address the DAT/SERT selectivity issue: the DAT-selective ligand methcathinone (MCAT), which lacks substituents on the aromatic ring, and the non-selective 4-iodomethcathinone (4-IMAP), which only differs in the *para* substituent at the aromatic moiety. A third ligand, mephe-drone (MEPH), was used to assess the agreement between computational and experimental findings (Figure 1).

The ligands were built in Molecular Operating Environment[17] (MOE) as the (*S*)-enantiomer in protonated form, while topolbuild (www.gromacs.org) was used to generate the GROMACS OPLS topology skeleton. The atom types were taken from the OPLS-AA/L[18] force field files and the
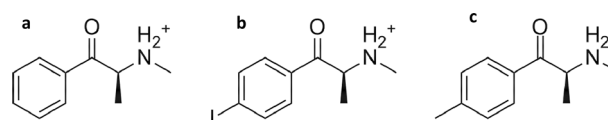

Figure 1. Structural formula of **a.** (*S*)-methcathinone (MCAT), **b.** (*S*)-4-iodomethcathinone (4-IMAP) and **c.** (*S*)-mephedrone (MEPH).

chiral α-carbon was assigned as a peptidic backbone carbon atom. The sigma hole of the iodine atom in 4-IMAP was represented by a virtual site with parameters described previously.[19] Missing dihedral parameters were taken from the OPLS2005 force field of Schrodinger,[20] while its transferability was confirmed by checking the remaining charges, bond lengths, angles and dihedral parameters.

2.4 Protein Preparation and Docking

From a previously published hDAT MD study of the *apo* form conducted by Stockner *et al*[21], a trajectory snapshot (taken at 17.6 ns of the production run) with sufficient space for an aromatic ring between Val152 and Ala423 (*B-site*)[8,12,22] was selected for docking the larger 4-IMAP ligand using GOLD 5.2,[23] following the procedure outlined in Ref.[12] Two different poses were obtained, which were placed back in the membrane system of the original trajectory.[21] In addition, 9 overlapping waters were removed.

The S1 site of SERT and DAT consists of at least eleven amino acids, of which 5 are identical (D79, Y156, F320, V328 and S422, based on the DAT sequence numbering). To investigate which residues contribute most to selectivity, those native to SERT were introduced *in silico* in the S1 site of DAT. Thus, three mutants were generated:

1. a V152I mutant, by placing the additional atoms into a void using MOE,

2. an octuple, *SERT-ized* mutant (designated as SERT-8mut), which comprises the F76Y, S149A, V152I, G153A, A423T, G425A, M427L, and S429G mutations in DAT. The G425A and S429G mutations are located slightly farther from the S1 site, but nonetheless were introduced based on *SERT-ized* leucine transporter crystal structures.[24] Additionally, the S429G mutation may prevent the formation of a hydrogen bond with the Tyr76 side chain in the S1 pocket native to SERT. Two possible starting conformations of Thr423 (in SERT-8mut) were generated, depending on the χ1 dihedral angle (approx. −80 and 160 degrees along C-C_α-C_β-C_γ).

3. a SERT-8mut-[I152 V] mutant, prepared from the SERT-8mut system after 140 ns of simulation.

2.5 Molecular Dynamics (MD) Simulations

The simulation systems, in addition to the *apo* structures, were parametrized for GROMACS using the OPLS-AA/L force field with settings described previously.[21] They contained approximately 9890 SPC water molecules,[25] 190

POPC lipid molecules[26] and 36 ions in the bulk solvent. Energy minimization was conducted using the steepest descent method with a convergence criterion of $10\,kJ\,mol^{-1}\,nm^{-1}$ and an initial step of 0.01 nm. The systems were equilibrated by gradually heating in four simulations of 1 ns, starting at 100 K using position restraints of $1000\,kJ\,mol^{-1}\,nm^{-2}$ for the protein-bound ions and the ligand and $100\,kJ\,mol^{-1}\,nm^{-2}$ for the backbone atoms, while decreasing the restraints by a factor of ten every simulation and increasing the temperature by 50 K. The systems then underwent a production run at 300 K until stability was achieved. The latter was evaluated by the following analyses: root mean-square (RMS) deviations of positions of the protein backbone atoms and the residues surrounding the ligand; the ligand-Asp79 salt bridge distance; Phe76/Tyr76 χ1 dihedral angles; and the potential energy of the system. Based on this, we decided to compare the trajectories of the first 100 ns. The complexes were run in duplicates or triplicates depending on the stability, using a different seed for the random starting velocities based on a Maxwell-Boltzmann distribution.

To identify the differences that lead to selectivity between SERT and DAT, the following protein-ligand interactions were monitored in all trajectories: the salt bridge strength, defined as the distance between the cationic nitrogen atom of the ligand and the C_γ atom of Asp79; stacking, defined as the distance between the centers of mass of the aromatic ring of the ligand and of Tyr156, Phe320 or Phe326; cation-π stacking, defined as the distance between the ligand's cationic nitrogen and the center of mass of the Phe76 (DAT) or Tyr76 (SERT-8mut) ring. Additionally, ligand atom-positional RMS fluctuations, and distances between the para-carbon of the ligand and Val343-C_β and Thr423-C_α atoms were monitored.

2.6 Thermodynamic Integration

To assess agreement with experimental findings, differences in binding free energies between the two ligands MCAT and MEPH were calculated using the thermodynamic integration (TI) method.[27] In addition, these calculations could further validate the adapted architecture of the SERT pocket, as well as the binding mode proposed.

In the TI method, a coupling parameter λ was introduced to make the Hamiltonian (H) λ-dependent such that at $\lambda =$ 0 or 1, H described two thermodynamic end states (A and B, respectively) of interest. The derivative of H with respect to a coupling parameter $\lambda (dH/d\lambda)$ was calculated at regular intervals. At every λ value, the uncertainty in $<dH/d\lambda>$ was evaluated by calculating the error estimate for the average (which reflects the adequacy of sampling) from the variance between block averages, using GROMACS' g_analyze tool with the error estimate option (ee)[28] The free energy difference (ΔG) between states A and B (as well as its error estimate) was yielded by integration:[29]

$$\Delta G_{A-B} = \int_{\lambda=0}^{1} \left\langle \frac{\partial H}{\partial \lambda} \right\rangle d\lambda$$

A thermodynamic cycle (Figure 2) was employed to obtain the difference $\Delta G_1 - \Delta G_2$ in SERT-8mut binding free energy between MCAT (1) and MEPH (2). Forward and backward ligand perturbations were performed for the unbound and protein-bound ligands to estimate ΔG_3 and
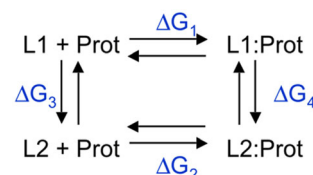
Figure 2. Thermodynamic cycle employed for the calculation of the difference in binding free energy between MCAT (L2) and MEPH (L1).

ΔG_4. For the ligand perturbations, a double topology paradigm was employed, whereby partial charges and Lennard-Jones (LJ) interaction sites of the para-hydrogen or para-methyl groups (of MCAT and MEPH, respectively) were simultaneously annihilated or created. Simulations were performed at $\lambda = 0$, 0.1, 0.2, …, 0.8, 0.9, 1.0 with a spacing of 0.05 between $\lambda = 0.2$ and $\lambda = 0.8$. At every λ value, at least 2.5 ns of simulation were performed and the equilibration time was kept at 1 ns. The simulation windows were run serially, i.e., the preceding final coordinates and velocities were used as starting point for the sequential window, to account for conformational changes and to obtain smooth $<dH/d\lambda>$ curves. To accelerate the calculation and to improve convergence of $<dH/d\lambda>$ and its error estimate, a simulation continued to the sequential window as soon as an error estimate of $<2\,kJ\,mol^{-1}$ was achieved and when the slope of the curve fitted to the error as a function of block size was $<0.1\,kJ\,mol^{-1}\,ns^{-1}$ for both the electrostatic (QQ) and LJ components of $<dH/d\lambda>$ (Figure 3). Ad-
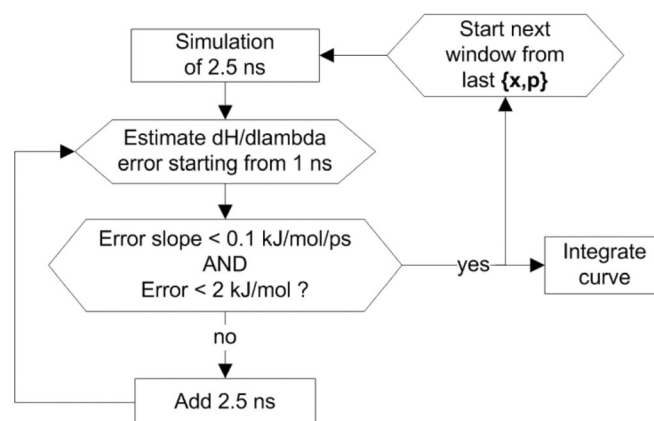
Figure 3. Applied scheme for the productions runs used for thermodynamic integration (TI).

These are not the final page numbers! ↗↗

ditionally, the LJ interactions were modified using a soft-core potential[30] with α_{sc} parameter of 0.5, to prevent singularities in $<dH/d\lambda>$ at λ values close to 0 and 1. All other simulation settings were identical to the MD settings described above. Reaching of the end state at $\lambda = 1$ was checked by evaluating time series for the Phe76/Tyr76 χ1 dihedral angle, the stacking distances between the ligand and Tyr156, Phe320 and Phe326, and the distance between the ligand's cationic nitrogen and the Phe/Tyr76 side chain center of mass of the phenyl ring.

For the perturbation of the unbound ligands, TI was performed with identical set-up and the ligands were simulated in simple point charge (SPC) water within a box with a distance of 2 nm to the box edges (circa 3270 water molecules). The $<dH/d\lambda>$ curves were obtained by simulating at 11 equally distributed windows of each 3 ns long, while discarding the first 500 ps for equilibration. The free energy difference between the end states was calculated using trapezoidal integration.

2.7 Biological Testing

To validate the results of the MD simulations, site-directed mutagenesis was performed on SERT using the Agilent(R) Quikchange Lightning kit. pEYFP-C1-hSERT wild-type DNA was used as template for the primers obtained from Agilent. The SERT-I172V reverse primer:

5'-GTGTTGTAGTAGGAAGCA**ACG**TAAAAGGCAATGATGCAG-3' was used, with the mutation indicated in bold. The new plasmids were sequenced and transformed into *Escherichia coli* XL10 Gold competent bacteria to obtain larger amounts.

HEK-293 cells were grown at 37 °C under a 5 % CO_2 and humid atmosphere in Dulbecco's Modified Eagle's medium (DMEM) supplemented with 10 % fetal calf serum and 1 % penicillin. Cells of approximately 80 % confluence were transiently transfected using Lipofectamine (Invitrogen) and seeded onto a poly-D-lysine coated 96-well plate while assuring approximately $8 \cdot 10^5$ cells/well for the subsequent day. The (*S*)-MCAT solution series was prepared as a stock of 100 mM in Krebs-HEPES buffer (KHB) and diluted stepwise for both the pre-incubation and uptake inhibition solutions. The uptake solution additionally contained 0.2 μM [³H]5-HT or [³H]-dopamine for the SERT and DAT measurements, respectively. The KHB for the DAT measurements additionally contained 100 μM paragyline and ascorbic acid to prevent metabolism and oxidation of the dopamine. After incubating MCAT in triplicate for 5 minutes, the solutions were replaced by 50 μL uptake solution for 60 seconds. The reaction was cooled down to 4 °C and the cells were lysed with 1 % sodium dodecyl sulphate (SDS) solution, followed by liquid scintillation counting. The counts were plotted using SigmaPlot after subtraction of the counts related to unspecific uptake at the highest MCAT concentration.

2.8 Statistical Analysis

Statistical analyses were carried out using GraphPad Prism (v. 5.0; GraphPad Scientific, San Diego, CA, USA). IC_{50} values for inhibition of uptake were calculated based on non-linear regression analysis.

3 Results and Discussion

3.1 Simulations Indicate that Cathinones Bind with their Carbonyl Group Directed toward Transmembrane Helix 6 in DAT and SERT

4-IMAP, the larger of the two ligands employed to study selectivity, was docked into the substrate binding site of the DAT homology model previously established.[21] Two different poses were obtained in which the ligand carbonyl group was either directed extracellularly (pose 1) or towards transmembrane helix (TM) 6 (pose 2, see Figure 4a). Wild-type DAT, DAT[V152I], SERT-*ized* DAT (SERT-8mut) and SERT-*ized* DAT[I152V] (SERT-8mut-[I152V]) were stable during MD simulations based on the analyses described in the Methods section, with pose 2 consistently showing an energetically more favorable protein-ligand interaction energy profile (see Figure 4b). Additionally, pose 2 simulations exhibited a more stable hydrogen bonding between the cationic nitrogen of the ligand and the Phe320 backbone, as compared to pose 1 (Figure S1a). This interaction was also observed in occluded co-crystallized LeuT structures between the amino group of leucine and the backbone oxygen atom of the homologous Phe253,[31] in addition to previous MD studies of DAT and SERT in complex with phenylethylamine substrates.[32–34] A transition from pose 1 to pose 2 was observed in the SERT-8mut/4-IMAP system as well, but not vice-versa. Therefore, the pose 2 simulations were used for assessing differences between SERT and DAT binding.

An additional finding was the hydrogen bond between the hydroxyl group of Thr423 in SERT-8mut and the Gly419 backbone carbonyl (Figure S1c).

3.2 Mephedrone inhibits SERT Uptake more than Methcathinone

Regarding the overlap of the core structures of MCAT and MEPH, the influence of a differential access path through the transporter could be considered negligible. Therefore, the binding free energy difference of these ligands for SERT ($\Delta\Delta G_{MEPH \rightarrow MCAT}$) can be calculated as 9.1 kJ mol^{-1} from dissociation and estimated inhibition constants using the Cheng-Prusoff equation:[35]

$$\frac{K_{D,MEPH}}{K_{D,MCAT}} \approx \frac{K_{i,MEPH}}{K_{i,MCAT}} = \frac{IC_{50,MEPH}}{IC_{50,MCAT}} \frac{\left(1 + \frac{[5HT]}{K_{D,5HT}}\right)}{\left(1 + \frac{[5HT]}{K_{D,5HT}}\right)} = \frac{IC_{50,MEPH}}{IC_{50,MCAT}},$$
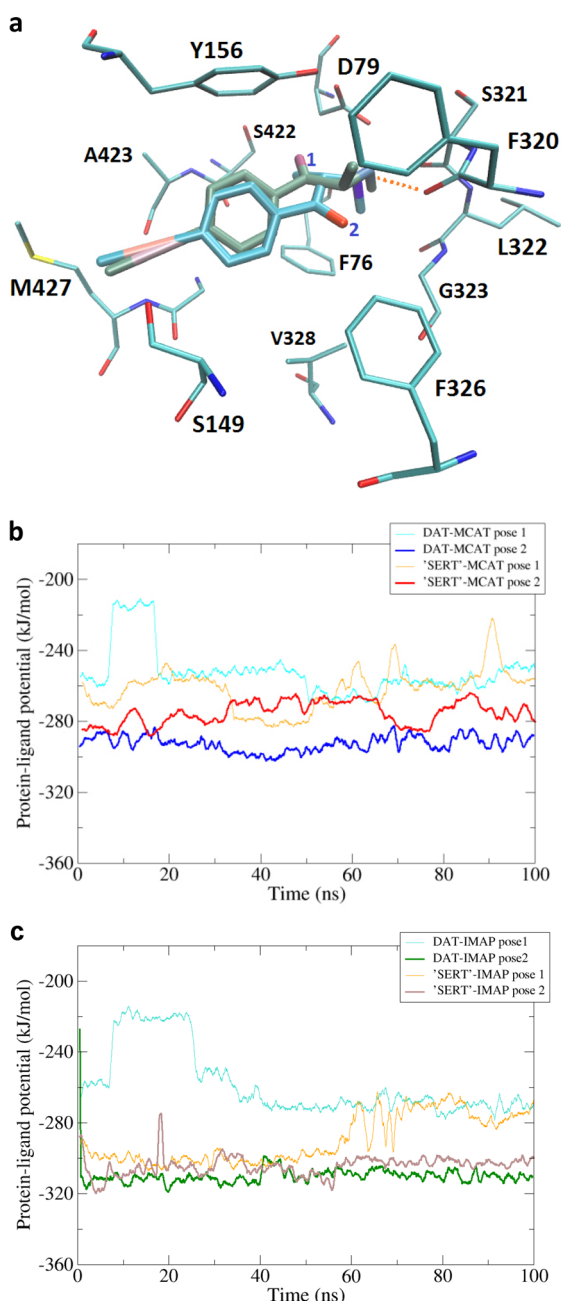
These are not the final page numbers! ↗↗

Figure 4. Two binding modes of 4-iodomethcathinone (4-IMAP) in the S1 site of the dopamine transporter obtained by docking. The 'atom' attached to the iodine atom represents the sigma hole, while the orange dotted line is a conserved hydrogen bond (a). Simulations starting from pose 2 generally showed more favorable protein-MCAT (b) and protein-4-IMAP (c) interaction energies than simulations starting from pose 1. The time series represent 2 ns running averages.

with $K_{D,5HT}$ being the dissociation constant of the radiolabeled serotonin substrate.

$$\Delta\Delta G_{\text{MEPH}\rightarrow\text{MCAT}} \approx -RT \ln \frac{IC_{50,\text{MEPH}}}{IC_{50,\text{MCAT}}} = +8.2 \pm 2.9 \text{ kJ mol}^{-1}$$

Hence, the *para*-methyl group of MEPH has a positive impact on SERT binding.

3.3 The Selectivity of SERT for Mephedrone over Methcathinone may Reside in the Substrate Binding Site

A TI calculation was performed in the DAT system with the SERT-like S1 pocket, to assess whether MEPH is predicted to bind stronger than MCAT to SERT, as shown by inhibition experiments.[36]

The simultaneous decoupling of the *para*-methyl group and the coupling of the *para*-hydrogen of MEPH in the complex yielded smooth $<dH/d\lambda>$ curves when employing λ steps of 0.05 between the simulation windows in the 'soft' states (with λ ranging from 0.2 to 0.8; see Figure S3 for the derivatives). The TI perturbation in the backward direction was performed by first modifying the LJ potentials before the electrostatic potentials to prevent numerical instabilities due to the growing charges of the methyl group. Therefore, $<dH/d\lambda>$ values for the protein-ligand complex calculations were slightly deviating between the forward and backward TI, but the hysteresis was relatively low (approximately 3 kJ mol^{-1}). Hence, the number of lambda steps used was considered adequate for this calculation. A difference in SERT-8mut binding free energy between MEPH and MCAT of $+10.8 \pm 1.2$ kJ mol^{-1} was obtained, which is within the error of the experimental value of $+8.2$ kJ ± 2.9 mol^{-1}. Hence we suggest that the SERT S1 site is substantially contributing to the difference in binding affinity between these two ligands.

3.4 DAT Selectivity for Ring-unsubstituted Amphetamines Seems Partly Caused by more Favorable Interactions with Phe320 in DAT as Compared to Phe355 in SERT, due to a Val/Ile Difference in the Central Binding Site

In the MD simulations, no evidence was found for differences in interaction between the ligand and other residues in the S1 site, except for the average distance between the aromatic ring of MCAT and Phe320. This distance was approximately 0.10 nm shorter in DAT, as compared to in SERT-8mut. At the same time, the distance between the non-selective 4-IMAP and Phe320 was similar in DAT and SERT-8mut (0.65 nm, see Figure 5a and 5b). The LJ potential between the ligand and Phe320 also showed clear differences (Figure 5c). These findings led to the hypothesis that the additional methyl group of Ile152 in SERT-8mut (Ile172 in SERT) hinders the aromatic interaction and therefore, simulations of the diagnostic mutants DAT-V152I and SERT-8mut-I152V served for proof of hypothesis. The observation in all 4-IMAP systems was the iodine atom being 'stuck' in the *B* pocket, preventing interaction with Phe320 in any case.

Based on uptake inhibitory assays, MCAT selectivity is around 50 fold for DAT over SERT(1.4 vs. 75.9 μM IC_{50}, respectively).
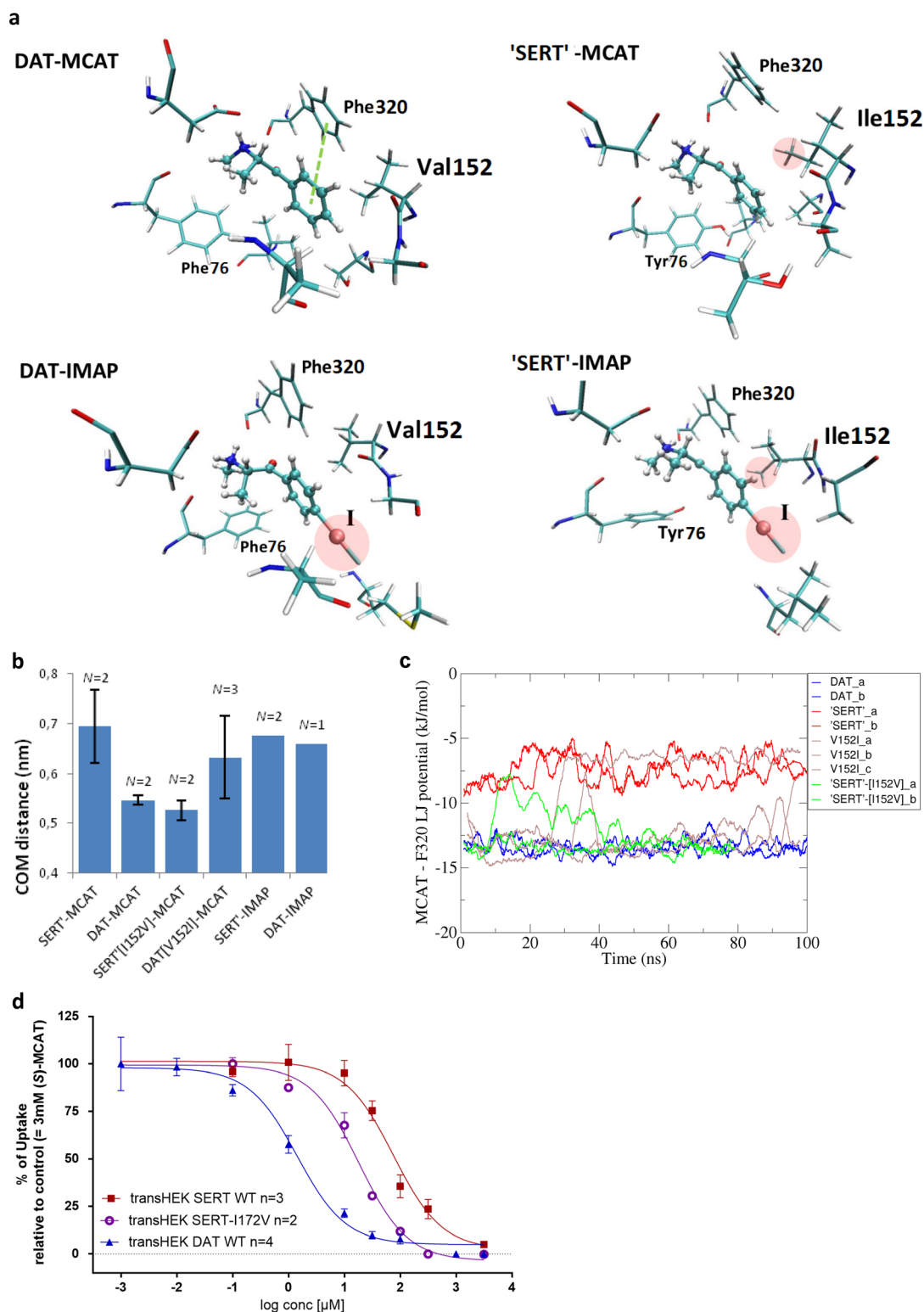
Figure 5. (a) Binding modes showing (*S*)-methcathinone (MCAT) interacting in the dopamine transporter (DAT) with Phe320 due to the lack of a *para*-substituent and due to Val152. SERThas an isoleucine at the homologous position preventing such an interaction. (b) Distances between the ligand and Phe320 rings show differences between Val and Ile containing proteins. (c) MCAT-Phe320 van der Waals energies showing the difference between SERT-8mut, DAT, the single mutant V152I and the SERT-8mut-[I152V] mutant. The DAT-[V152I] energies were less reproducible as compared to the other systems, due to the occurrence of new binding site architectures. Back-mutating from Ile to Val in SERT-8mut clearly shows a recovery of the interaction between the ligand and Phe320. (d) Uptake inhibition curves of SERT-[I172V] in the serotonin and dopamine transporter transiently expressed in HEK-293 cells showing a 4x increase in activity of the DAT-like SERT-[I172 V] mutant. Error bars represent the standard error of the mean (SEM).

The uptake inhibitory activity of MCAT in the SERT-I172V mutant was indeed increased significantly to 18.3 µM IC_{50} (Figure 5d). The results therefore indicate that increased space due to the Ile-to-Val mutation led to improved protein-ligand interactions and hence provides an explanation for the DAT-over-SERT selectivity of ring-unsubstituted cathinones.

4 Conclusions

Molecular dynamics simulations are a versatile tool for obtaining insights into ligand-protein interactions. Exploiting this method on the neurotransmitter transporter DAT and a *SERT-ized* DAT (SERT-8mut) provided hypotheses, which allowed a more detailed understanding of the protein-ligand interactions and protein pocket flexibility. Simulating the ligands MCAT and 4-IMAP in an occluded model of DAT and *SERT-ized* DAT indicates that the ligand's conformation with the carbonyl group directed toward TM6 is enthalpically more favorable and shows more stable hydrogen bonding between the ligand and the protein. This is in agreement with previous studies employing dopamine and 3,4-methylenedioxymethamphetamine (MDMA).

Due to the hydrogen bond between the hydroxyl group of Thr423 and the Gly419 backbone in SERT-8mut (Thr439 in SERT) the Thr methyl group was directed towards the ligand binding site. This has implications for the hydrophobicity of the pocket and may explain the higher affinity of *para*-methylated ligands in SERT.

A closer understanding of DAT-over-SERT selectivity of small amphetamines was accomplished by the differences observed in ligand-protein aromatic interactions, which were more favorable in DAT. This was presumably due to a less bulky Val152 residue compared to Ile172 in SERT, which can hinder such interactions. The simulations were validated by uptake inhibitory assays in which an increase in activity was observed for the DAT-like SERT-I172 V mutant. These results show that subtle differences in the interaction pattern of cathinones drive their transporter selectivity.

Conflict of Interest

None declared.

Acknowledgements

References

[1] K. P. Lesch, C. S. Aulakh, B. L. Wolozin, D. L. Murphy, *Pharmacol. Toxicol.* **1992**, *71 Suppl 1*, 49–60.

[2] K. P. Lesch, D. Bengel, A. Heils, S. Z. Sabol, B. D. Greenberg, S. Petri, J. Benjamin, C. R. Muller, D. H. Hamer, D. L. Murphy, *Science* **1996**, *274*, 1527–1531.

[3] N. J. van der Wee, H. Stevens, J. A. Hardeman, R. C. Mandl, D. A. Denys, H. J. van Megen, R. S. Kahn, H. M. Westenberg, *A . J. Psychiatry* **2004**, *161*, 2201–2206.

[4] L. Kent, U. Doerry, E. Hardy, R. Parmar, K. Gingell, Z. Hawi, A. Kirley, N. Lowe, M. Fitzgerald, M. Gill, N. Craddock, *Mol. Psychiatry* **2002**, *7*, 908–912.

[5] F. A. Baughman, *The Lancet* **2000**, *355*, 1460–1461.

[6] S. Agatonovic-Kustrin, P. Davies, J. Turner, *Medicinal Chemistry* **2009**, *5*, 271–278.

[7] E. Greiner, T. L. Boos, T. E. Prisinzano, M. G. De Martino, B. Zeglis, C. M. Dersch, J. Marcus, J. S. Partilla, R. B. Rothman, A. E. Jacobson, K. C. Rice, *J. Med. Chem.* **2006**, *49*, 1766–1772.

[8] A. Seddik, M. Holy, R. Weissensteiner, B. Zdrazil, H. H. Sitte, G. F. Ecker, *Mol. Inf.* **2013**, *32*, 409–413.

[9] W. A. James, S. Lippmann, *Southern Medical Journal* **1991**, *84*, 222–224.

[10] N. V. Cozzi, D. Marona-Lewicka, D. E. Nichols, A. Gokin, K. F. Foley, *Soc Neurosci Abs.* **2005**, *31*, 533-35.

[11] A. Shiozawa, K. Narita, G. Izumi, S. Kurashige, K. Sakitama, M. Ishikawa, *Eur. J. Med. Chem.* **1995**, *30*, 85–94.

[12] K. Saha, J. S. Partilla, K. R. Lehner, A. Seddik, T. Stockner, M. Holy, W. Sandtner, G. F. Ecker, H. H. Sitte, M. H. Baumann, *Neuropsychopharmacology* **2014**, *40*, 1321–1331.

[13] A. Seddik, T. Steinkellner, T. Stockner, W. Sandtner, M. Freissmuth, H. H. Sitte, G. F. Ecker, in *American Chemical Society Meeting, COMP division, Pub #443, San Francisco 2014*.

[14] T. Hofmaier, A. Luf, A. Seddik, T. Stockner, M. Holy, M. Freissmuth, G. F. Ecker, R. Schmid, H. H. Sitte, O. Kudlacek, *Neurochem. Int.* **2014**, *73*, 32–41.

[15] J. A. Schmid, P. Scholze, O. Kudlacek, M. Freissmuth, E. A. Singer, H. H. Sitte, *J. Biol. Chem.* **2000**, *276*, 3805–3810.

[16] K. F. Foley, N. V. Cozzi *Drug Dev. Res.* **2003**, *60*, 252–260.

[17] C. C. G. I. Molecular Operating Environment (MOE), 1010 Sherbooke St. West, Suite #910, Montreal, QC, Canada, H3A 2R7, 2013.

[18] G. A. Kaminski, R. A. Friesner, J. Tirado-Rives, W. L. Jorgensen, *Phys. Chem. B* **2001**, *105*, 6474–6487.

[19] W. L. Jorgensen, P. Schyman, *J. Chem. Theory Comput.* **2012**, *8*, 3895–3901.

[20] J. L. Banks, H. S. Beard, Y. Cao, A. E. Cho, W. Damm, R. Farid, A. K. Felts, T. A. Halgren, D. T. Mainz, J. R. Maple, R. Murphy, D. M. Philipp, M. P. Repasky, L. Y. Zhang, B. J. Berne, R. A. Friesner, E. Gallicchio, R. M. Levy, *J. Comput. Chem.* **2005**, *26*, 1752–1780.

[21] T. Stockner, T. R. Montgomery, O. Kudlacek, R. Weissensteiner, G. F. Ecker, M. Freissmuth, H. H. Sitte, *PLoS Comput Biol* **2013**, *9*, e1002909.

[22] J. Andersen, L. Olsen, K. B. Hansen, O. Taboureau, F. S. Jorgensen, A. M. Jorgensen, B. Bang-Andersen, J. Egebjerg, K. Stromgaard, A. S. Kristensen, *J. Biol. Chem.* **2009**, *285*, 2051–2063.

[23] G. Jones, P. Willett, R. C. Glen, A. R. Leach, R. Taylor, *J. Mol. Biol.* **1997**, *267*, 727–748.

[24] H. Wang, A. Goehring, K. H. Wang, A. Penmatsa, R. Ressler, E. Gouaux, *Nature* **2013**, *503*, 141–145.

[25] H. J. C. Berendsen, J. P. M. Postma, W. F. van Gunsteren, J. Hermans, in *The Jerusalem Symposia on Quantum Chemistry and*

Biochemistry, Springer Science + Business Media, **1981**, pp. 331–342.

[26] O. Berger, O. Edholm, F. Jähnig, *Biophys. J.* **1997**, *72*, 2002–2013.

[27] D. L. Beveridge, F. M. DiCapua, *Annu. Rev. Biophys. Biophys. Chem.* **1989**, *18*, 431–492.

[28] B. Hess, *J. Chem. Phys.* **2002**, 116, 209.

[29] J. G. Kirkwood, *J. Chem. Phys.* **1935**, *3*, 300.

[30] T. C. Beutler, A. E. Mark, R. C. van Schaik, P. R. Gerber, W. F. van Gunsteren, *Chem. Phys. Lett.* **1994**, *222*, 529–539.

[31] A. Yamashita, S. K. Singh, T. Kawate, Y. Jin, E. Gouaux, *Nature* **2005**, *437*, 215–223.

[32] T. Beuming, J. Kniazeff, M. L. Bergmann, L. Shi, L. Gracia, K. Raniszewska, A. H. Newman, J. A. Javitch, H. Weinstein, U. Gether, C. J. Loland, *Nat. Neurosci.* **2008**, *11*, 780–789.

[33] K. Severinsen, J. F. Kraft, H. Koldsø, K. A. Vinberg, R. B. Rothman, J. S. Partilla, O. Wiborg, B. Blough, B. Schiøtt, S. Sinning, *ACS Chem. Neurosci.* **2012**, *3*, 693–705.

[34] H. Koldsø, A. B. Christiansen, S. Sinning, B. Schiøtt, *ACS Chem. Neurosci.* **2013**, *4*, 295–309.

[35] C. Yung-Chi, W. H. Prusoff, *Biochem. Pharmacol.* **1973**, *22*, 3099–3108.

[36] A. J. Eshleman, K. M. Wolfrum, M. G. Hatfield, R. A. Johnson, K. V. Murphy, A. Janowsky, *Biochem. Pharmacol.* **2013**, *85*, 1803–1815.

These are not the final page numbers! ↗↗
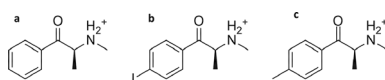
A. Seddik, D. P. Geerke, T. Stockner, M. Holy, O. Kudlacek, N. V. Cozzi, A. E. Ruoho, H. H. Sitte, G. F. Ecker*

■■ – ■■

Combined Simulation and Mutation Studies to Elucidate Selectivity of Unsubstituted Amphetamine-like Cathinones at the Dopamine Transporter